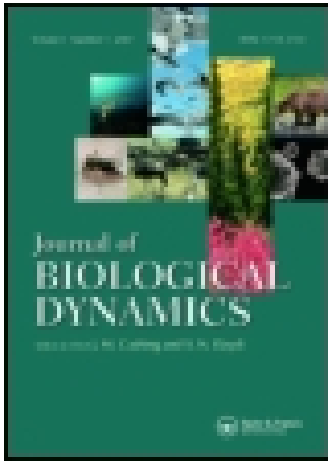


This article was downloaded by: [University of Alberta]

On: 08 September 2014, At: 14:50

Publisher: Taylor & Francis

Informa Ltd Registered in England and Wales Registered Number: 1072954 Registered office: Mortimer House, 37-41 Mortimer Street, London W1T 3JH, UK



Journal of Biological Dynamics

Publication details, including instructions for authors and subscription information:

<http://www.tandfonline.com/loi/tjbd20>

Birth-jump processes and application to forest fire spotting

T. Hillen^a, B. Greese^b, J. Martin^a & G. de Vries^a

^a Department of Mathematical and Statistical Sciences, Centre for Mathematical Biology, University of Alberta, Edmonton, Canada

^b Department of Astronomy and Theoretical Physics, Computational Biology and Biological Physics, Lund University, Lund, Sweden

Published online: 04 Sep 2014.

To cite this article: T. Hillen, B. Greese, J. Martin & G. de Vries (2014): Birth-jump processes and application to forest fire spotting, Journal of Biological Dynamics, DOI: [10.1080/17513758.2014.950184](https://doi.org/10.1080/17513758.2014.950184)

To link to this article: <http://dx.doi.org/10.1080/17513758.2014.950184>

PLEASE SCROLL DOWN FOR ARTICLE

Taylor & Francis makes every effort to ensure the accuracy of all the information (the "Content") contained in the publications on our platform. Taylor & Francis, our agents, and our licensors make no representations or warranties whatsoever as to the accuracy, completeness, or suitability for any purpose of the Content. Versions of published Taylor & Francis and Routledge Open articles and Taylor & Francis and Routledge Open Select articles posted to institutional or subject repositories or any other third-party website are without warranty from Taylor & Francis of any kind, either expressed or implied, including, but not limited to, warranties of merchantability, fitness for a particular purpose, or non-infringement. Any opinions and views expressed in this article are the opinions and views of the authors, and are not the views of or endorsed by Taylor & Francis. The accuracy of the Content should not be relied upon and should be independently verified with primary sources of information. Taylor & Francis shall not be liable for any losses, actions, claims, proceedings, demands, costs, expenses, damages, and other liabilities whatsoever or howsoever caused arising directly or indirectly in connection with, in relation to or arising out of the use of the Content.

This article may be used for research, teaching, and private study purposes. Terms & Conditions of access and use can be found at <http://www.tandfonline.com/page/terms-and-conditions>

It is essential that you check the license status of any given Open and Open Select article to confirm conditions of access and use.

Birth-jump processes and application to forest fire spotting

T. Hillen^{a*}, B. Greese^b, J. Martin^a and G. de Vries^a

^aDepartment of Mathematical and Statistical Sciences, Centre for Mathematical Biology, University of Alberta, Edmonton, Canada; ^bDepartment of Astronomy and Theoretical Physics, Computational Biology and Biological Physics, Lund University, Lund, Sweden

(Received 9 March 2014; accepted 25 July 2014)

Birth-jump models are designed to describe population models for which growth and spatial spread cannot be decoupled. A birth-jump model is a nonlinear integro-differential equation. We present two different derivations of this equation, one based on a random walk approach and the other based on a two-compartmental reaction–diffusion model. In the case that the redistribution kernels are highly concentrated, we show that the integro-differential equation can be approximated by a reaction–diffusion equation, in which the proliferation rate contributes to both the diffusion term and the reaction term. We completely solve the corresponding critical domain size problem and the minimal wave speed problem. Birth-jump models can be applied in many areas in mathematical biology. We highlight an application of our results in the context of forest fire spread through spotting. We show that spotting increases the invasion speed of a forest fire front.

Keywords: birth-jump processes; integro-differential equations; diffusion limit; reaction–diffusion equations; critical domain size; minimal wave speed; wildfire spotting

AMS Classification: 92B05, 35Q92, 45K05

1. Introduction

Typical mathematical models for spatial spread of growing and interacting populations assume that growth and spatial spread are independent processes. For example, one typically models the evolution of a population that undergoes diffusion and logistic growth with the Fisher equation

$$u_t = Du_{xx} + \mu u \left(1 - \frac{u}{C}\right),$$

where $u(x, t)$ denotes the population density at time t and location x , D is a constant diffusion coefficient, and the nonlinearity $\mu u(1 - u/C)$ describes logistic growth with growth rate $\mu > 0$ and carrying capacity $C > 0$.

In many situations, however, growth and spread cannot be decoupled as in the model above. For example, ovarian cancer in advanced stages sheds new cancer cells into the peritoneal cleavage. These cancer cells are transported by the peritoneal fluid to distant locations, possibly

*Corresponding author. Email: thillen@ualberta.ca

Author Emails: bettina.greese@thep.lu.se; jmartin2@ualberta.ca; gerda.devries@ualberta.ca

starting metastatic growth. Here, the spatial spread of cells is directly related to cell division [6,37]. Similar examples include any form of metastasis that results from shedding of tumour cells into the blood stream. A different example is the spread of wildfires, where burning embers are released into the wind and transported downwind. If not extinguished during flight, they might start a new fire ahead of the main fire front; this process is called *spotting* [1,28]. Yet another example is that of a territorial species, where young individuals are forced to leave the pack and find their own territories.

In this paper, we discuss models that are suitable to describe situations in which growth and spread cannot be decoupled. These models arise from what we call *birth-jump processes* and their corresponding *birth-jump partial differential equations; PDEs*. The birth-jump processes are generalizations of *position-jump processes* as discussed, for example, in [18,31] on the one hand and of reaction–diffusion models on the other hand [36].

In its general form, for the density of one population, $u(x, t)$, the birth-jump integro-differential equation in a given domain $\Omega \subset \mathbb{R}^n$ can be written as

$$\begin{aligned}
 u_t(x, t) = & \underbrace{\int_{\Omega} K(x, y, u(x, t)) \alpha(u(y, t)) u(y, t) \, dy}_{\text{position-jump process}} - \alpha(u(x, t)) u(x, t) \\
 & + \underbrace{\int_{\Omega} S(x, y, u(x, t)) \beta(u(y, t)) u(y, t) \, dy}_{\text{birth-jump process}} - \underbrace{\delta(u(x, t)) u(x, t)}_{\text{death}}. \quad (1)
 \end{aligned}$$

The first two terms describe a nonlinear position-jump process, where $\alpha(u)$ is the rate for an individual to leave location x . The kernel K is a redistribution kernel representing the probability density of an individual to jump from y to x , conditioned on the local occupancy at x given by $u(x, t)$. The dependence of K on $u(x, t)$ can be used to model volume constraints, such that new individuals can only arrive at x if there is space available [17]. The third term is new, and it describes the proper birth-jump process. The function $\beta(u)$ is a proliferation rate at location y , and S is the redistribution kernel for newly generated individuals at y to jump to x . The birth-jump process does not lead to a negative term in the equations since it acts on newly generated individuals only. The transport mechanisms for existing individuals and for newly generated individuals may be the same, as in the case of metastatic cancer spread, implying $K = S$. This is different for forest fire spread, where local spread happens through convection, conduction and diffusion, while long-range spotting occurs through wind transport [21], hence $K \neq S$ in that case. The last term in Equation (1) is a standard death term with the death rate $\delta(u)$. To introduce notation that is used later, we combine the terms related to population growth and death as

$$f(u) = (\beta(u) - \delta(u))u \quad (2)$$

with $\beta, \delta \geq 0$.

Lutscher [25] studied a similar idea for a discrete-time integro-difference spread model. In [25], it is assumed that a fraction g of new-born individuals stays stationary, while the other fraction $1 - g$ is distributed according to a redistribution kernel. Lutscher computes spreading speeds for this case using moment-generating functions.

In Section 2, we present two derivations of the birth-jump process leading to Equation (1): one from a discrete random walk and another from a system of reaction–diffusion equations. In Section 3, we use moment expansions of the integral terms in Equation (1) to derive corresponding generalized reaction–diffusion equations. We show that it is important to choose the relocation rate $\alpha(u)$ and the proliferation rate $\beta(u)$ carefully to ensure that the diffusion limit is well defined. We then consider two standard problems for the diffusion limit, namely the critical

domain size problem and the travelling wave problem. Under very general suitable assumptions, we can fully characterize the critical domain size and the invasion speed. In Section 4, we discuss an application of our model to forest fire spotting. Spotting describes the launch of burning material into the wind column, its transport ahead of the fire, its landing, and the subsequent ignition of a new fire. Spotting is an important factor of wildfire spread, and new models that take the spotting phenomenon into account are needed. We use the birth-jump framework to develop models for spotting, and we apply the results from Section 3 to determine critical domain size and invasion speed. Our model predicts that spotting increases fire spread. We conclude with Section 5, where we argue that birth-jump models can be a useful tool in a wide variety of biological situations, from cancer metastasis to habitat selection and the *ideal free distribution* (IFD). We also discuss interesting mathematical questions that arise in the context of birth-jump processes.

2. Derivations of the birth-jump process

We use two different approaches¹ to derive our birth-jump model, both times arriving at the same type of integro-differential equation (1). In Section 2.1, we present the random walk approach. This first derivation is very general. In Section 2.2, we present a derivation via a two-compartmental reaction–diffusion model. This second derivation leads to very specific redistribution kernels K and S . For ease of discussion, we cast both derivations of the birth-jump process in the context of cell populations; the resulting equation can be interpreted more broadly, for example in terms of firebrands or populations of animals, depending on the application.

2.1. Derivation from a random walk

In order to model the birth-jump process, we imagine the domain of interest as an infinite line so that the model will be one dimensional. A similar derivation for a space-jump process is found in [18], however, the birth-jump process is not included there. We first discretize time into disjoint intervals of length Δt that cover the non-negative real line and discretize space into disjoint patches of size Δx that cover the whole real line. Each time step is represented by $t = n\Delta t$, and all patches are represented by integers $i, j \in \mathbb{Z}$. Let $u_i(t)$ be the number of cells at location i at time t . We imagine that this number changes over time due to spatial movement (shedding and settlement) as well as population dynamics (birth and death/survival). Hence, a descriptive equation for the number of cells in one patch is as follows:

$$\begin{aligned} \text{cells at time } t + \Delta t = & - \text{leaving cells} \\ & + \text{arriving cells} \\ & + \text{new-born cells} \\ & + \text{surviving cells from time } t, \end{aligned}$$

where the four terms on the right-hand side arise from the four concepts shedding, settlement, proliferation, and survival, respectively.

The ‘shedding’ term counts the cells that leave location i :

$$- \tilde{\alpha}(u_i(t))u_i(t), \tag{3}$$

where $\tilde{\alpha}(u_i(t))$ is the shedding probability.

The complementary ‘settlement’ term counts the cells that leave locations j and arrive at location i :

$$\sum_{j=-\infty}^{+\infty} \tilde{\alpha}(u_j(t))k_{ij}u_j(t), \quad (4)$$

where k_{ij} denotes the probability of a cell that was released at location j to settle at location i . Here, we implicitly assume that the release $\tilde{\alpha}$ and transport k_{ij} are independent processes. At this stage, we could allow the transport kernel to depend on occupancy at the target site, that is, $k_{ij} = k_{ij}(u_i)$.

The ‘proliferation’ term counts the cells that are born at locations j , leave j , and arrive at location i :

$$\sum_{j=-\infty}^{+\infty} \tilde{\beta}(u_j(t))s_{ij}u_j(t), \quad (5)$$

where $\tilde{\beta}(u_j(t))$ is the probability that a cell at j divides into two daughter cells during the time interval $[t, t + \Delta t)$. An important assumption in this context is that one daughter cell moves to some location i , while the other daughter cell replaces the mother. Consequently, the fate of the latter is governed by the shedding and settlement terms and does not affect the proliferation term. For the leaving daughter cells, we use the transitional probabilities s_{ij} . Depending on the application, the redistributions might be imperfect, i.e. cells might get lost. Hence, we assume $k_{ij}, s_{ij} \geq 0$ and the sums $\sum_{j=-\infty}^{+\infty} k_{ij}, \sum_{j=-\infty}^{+\infty} s_{ij} \leq 1$.

Finally, we need to count the individuals that stay at location i . The ‘survival’ term is

$$(1 - \tilde{\delta}(u_i(t)))u_i(t), \quad (6)$$

where $\tilde{\delta}(u_i(t))$ is the death rate.

Adding the terms (3)–(6) leads to the difference equation

$$u_i(t + \Delta t) - u_i(t) = \sum_{j=-\infty}^{+\infty} \tilde{\alpha}(u_j(t))k_{ij}u_j(t) - \tilde{\alpha}(u_i(t))u_i(t) + \sum_{j=-\infty}^{+\infty} \tilde{\beta}(u_j(t))s_{ij}u_j(t) - \tilde{\delta}(u_i(t))u_i(t). \quad (7)$$

The first two terms on the right-hand side of Equation (7) represent a standard discrete position-jump process (e.g. as discussed in [31]), the third term describes a discrete birth-jump process, and the last term describes cell death.

We now convert the discrete model into a continuous model. This is done by taking the limit as the time and space intervals become small and interpreting the sums in Equation (7) as integrals. Hence, the result has the form of an integro-differential equation. We let $x = i\Delta x$ and $y = j\Delta x$ and introduce a continuous population density $u(x, t)$ via

$$u(x, t)\Delta x = u_i(t),$$

rates $\alpha(u)$, $\beta(u)$, and $\delta(u)$ via

$$\alpha(u(x, t))\Delta t = \tilde{\alpha}(u_i(t)), \quad \beta(u(x, t))\Delta t = \tilde{\beta}(u_i(t)), \quad \delta(u(x, t))\Delta t = \tilde{\delta}(u_i(t)),$$

and redistribution kernels

$$K(x, y)\Delta x = k_{ij}, \quad S(x, y)\Delta x = s_{ij}.$$

Converting the discrete variables in Equation (7) into continuous ones yields the equation

$$\begin{aligned} (u(x, t + \Delta t) - u(x, t))\Delta x = & \sum_{j=-\infty}^{+\infty} \alpha(u(y, t))K(x, y)u(y, t)\Delta x^2\Delta t - \alpha(u(x, t))u(x, t)\Delta x\Delta t \\ & + \sum_{j=-\infty}^{+\infty} \beta(u(y, t))S(x, y)u(y, t)\Delta x^2\Delta t - \delta(u(x, t))u(x, t)\Delta x\Delta t. \end{aligned} \quad (8)$$

It should be noted that for $\beta = 0$, the equation coincides with Equation (5) in [18]. We cancel Δx , divide by Δt , and consider the limit as $\Delta x, \Delta t \rightarrow 0$. The sums in Equation (8) are Riemann sums, which converge to integrals. We obtain model (1) in one dimension, which reads

$$\begin{aligned} u_t(x, t) = & \int_{-\infty}^{+\infty} K(x, y)\alpha(u(y, t))u(y, t)dy - \alpha(u(x, t))u(x, t) \\ & + \int_{-\infty}^{+\infty} S(x, y)\beta(u(y, t))u(y, t)dy - \delta(u(x, t))u(x, t). \end{aligned} \quad (9)$$

Finally, if we use the analogous model in higher dimensions on a given domain $\Omega \subset \mathbb{R}^n$ and allow the integration kernels to depend on the local density u , then we obtain model (1).

Remarks

- (1) The derivation in this subsection is unchanged if we allow the kernels k_{ij} and s_{ij} to depend on u_i .
- (2) If volume constraints are important, then we often write the kernel in product form, i.e. $K(x, y, u(x, t)) = \kappa(x, y)\Psi(u(x, t))$, where $\kappa(x, y)$ is a redistribution kernel, and $\Psi(u)$ is a decreasing function in u [7].

2.2. Derivation from a reaction–diffusion system

We can use a system of two reaction–diffusion equations to derive model (1) for a particular kernel. The system describes the shedding of cells with two classes, namely a class $u(x, t)$ for stationary cells and a class $w(x, t)$ for cells that are transported. We assume that cell division occurs only in the stationary phase (since nutrients are available), but newly created cells are shed and transported immediately. The equation for u thus describes cell kinetics (birth and death), while the equation for w describes redistribution of the cells. We follow the ideas of Lutscher *et al.* [27] and assume that movement is fast relative to reproduction. The second equation is then in a quasi-steady state, and we solve it using the corresponding Green's function. This Green's function then leads to non-local terms in the first equation.

Let $\Omega \subset \mathbb{R}^n$ be an open domain. If Ω is bounded, then we assume a piecewise smooth boundary $\partial\Omega$ and assume that the density of moving cells at the boundaries is zero, i.e. $w(x, t) = 0$ on $\partial\Omega$. Based on our assumptions, we construct the following equations for the stationary class $u(x, t)$ and the mobile class $w(x, t)$:

$$\begin{aligned} u_t(x, t) = & -\alpha(u(x, t))u(x, t) + \eta(x)w(x, t) - \delta(u(x, t))u(x, t), \\ \tau w_t(x, t) = & (\Delta - \eta(x))w(x, t) + \alpha(u(x, t))u(x, t) + \beta(u(x, t))u(x, t), \end{aligned} \quad (10)$$

where Δ is the Laplace operator, representing diffusive cell movement, $\alpha(u)$ is the shedding rate, $\eta(x)$ is a spatially dependent rate of settlement, $\delta(u)$ is the death rate, and $\beta(u)$ the mitosis rate.

Note that newly created individuals enter the mobile class immediately. The variable τ is a time-scaling parameter which indicates that population growth and spread might act on different time scales. Since we assume that diffusion is fast compared to mitosis, we can replace the second equation in (10) by

$$-(\Delta - \eta(x))w(x, t) = (\alpha(u(x, t)) + \beta(u(x, t)))u(x, t). \quad (11)$$

If $\Omega = \mathbb{R}^n$, then Green's function is the standard normal distribution in \mathbb{R}^n . If Ω is a bounded domain with smooth boundary, then we denote by $G(x, y)$ Green's function of the elliptic problem

$$\begin{aligned} -(\Delta - \eta(x))w(x) &= \delta_x && \text{in } \Omega, \\ w(x) &= 0 && \text{on } \partial\Omega. \end{aligned}$$

Using this Green's function [10], we can write the solution of Equation (11) as

$$w(x, t) = \int_{\Omega} G(x, y)(\alpha(u(y, t)) + \beta(u(y, t))) u(y, t) dy.$$

If we substitute this expression for w into the first equation of (10), then we obtain

$$\begin{aligned} u_t(x, t) &= \int_{\Omega} \eta(x)G(x, y)\alpha(u(y, t))u(y, t) dy - \alpha(u(x, t))u(x, t) \\ &\quad + \int_{\Omega} \eta(x)G(x, y)\beta(u(y, t))u(y, t) dy - \delta(u(x, t))u(x, t), \end{aligned}$$

which is in fact (1) with $K(x, y) = S(x, y) = \eta(x)G(x, y)$.

3. Reaction–diffusion limit

In this section, we focus on the case in which the birth-jump process has concentrated kernels K and S , and we study approximations of the birth-jump equation (1). A moment expansion of the integral terms allows us in Section 3.1 to derive a diffusion limit (17), which is a nonlinear generalization of the well-known Fisher–KPP reaction–diffusion equation. The analysis of the critical domain size problem and the travelling wave problem are common methods for reaction–diffusion equations of the Fisher–KPP type [39], but both problems have not been studied for our limit Equation (17). In the critical domain size problem, discussed in Section 3.2, one is interested in finding the smallest habitat able to sustain a stable population. In the case of the travelling wave problem, discussed in Section 3.3, one is interested in how quickly a population would invade into an uninhabited habitat. We are able to find complete solutions for these two problems.

3.1. Derivation of the diffusion limit

In Section 3.1.1, we derive a nonlinear diffusion limit (17) through a moment expansion. In Section 3.1.2, we investigate an important special case, namely the case of a pure birth-jump process which has no spontaneous travel and where spread is only via newborns. In Section 3.1.3, we review a few specific growth models that will be used later to highlight key results.

3.1.1. General case

A diffusion limit can be obtained for concentrated kernels K and S by using a moment expansion of the integral terms. We assume that a given function $h(y, t)$ is analytic so that we can use the Taylor series expansion of $h(y, t)$ about $y = x$. For kernel K , rewriting the integral operator leads to

$$\begin{aligned} \int_{\Omega} K(x, y)h(y, t) \, dy &= \int_{\Omega} K(x, y) \sum_{i=0}^{+\infty} \frac{h^{(i)}(x, t)}{i!} (y - x)^i \, dy \\ &= \sum_{i=0}^{+\infty} h^{(i)}(x, t)M_i^K(x), \end{aligned} \tag{12}$$

where the term $h^{(i)}$ denotes the i th partial spatial derivative of h , and $M_i^K(x)$ is the i th moment of K defined as

$$M_i^K(x) := \int_{\Omega} K(x, y) \frac{(y - x)^i}{i!} \, dy. \tag{13}$$

The i th moment of S , $M_i^S(x)$, is defined analogously. We assume that these moments exist at least up to order 2. Note that if the kernel is symmetric in the sense that $K(x, x + z) = K(x, x - z)$, then all odd moments are zero. When, in addition, the kernel is sufficiently local, then the higher moments are small, and we can truncate the sum in Equation (12) after the third-order or fifth-order term without losing much precision. Hence, for a symmetric kernel K , the moment expansion formula is

$$\int_{\Omega} K(x, y)h(y, t) \, dy \approx M_0^K(x)h(x, t) + M_2^K(x)h_{xx}(x, t) \tag{14}$$

or

$$\int_{\Omega} K(x, y)h(y, t) \, dy \approx M_0^K(x)h(x, t) + M_2^K(x)h_{xx}(x, t) + M_4^K(x)h_{xxxx}(x, t). \tag{15}$$

Analogous moment expansion formulas can be written for a symmetric kernel S . In the following, we mostly use the second-order expansions.

We now include the density dependence of the integration kernels and use these moment expansions in the birth-jump process (1) to obtain

$$\begin{aligned} u_t &= M_2^K(x, u)(\alpha(u)u)_{xx} + M_2^S(x, u)(\beta(u)u)_{xx} \\ &\quad + (M_0^K(x, u) - 1)\alpha(u)u + (M_0^S(x, u)\beta(u) - \delta(u))u, \end{aligned} \tag{16}$$

which is the birth-jump PDE corresponding to Equation (1).

An interesting special case arises if we assume that there is no volume effect, i.e. K and S do not depend on u , that K and S are mass conserving, and that they only depend on the distance $x - y$ but not on the location x . Then, $M_0^K = 1$, $M_0^S = 1$, $M_2^K = d_K = \text{const}$, and $M_2^S = d_S = \text{const}$. Equation (16) then reduces to a generalization of the Fisher-KPP reaction-diffusion equation, namely

$$u_t = ((d_K\alpha(u) + d_S\beta(u))u)_{xx} + (\beta(u) - \delta(u))u. \tag{17}$$

Notice that in Equation (17), the birth rate β arises both in the diffusion term as well as in the kinetic term, whereas the death rate contributes to the kinetic term only. In the next sections, we analyse this nonlinear reaction-diffusion model in detail to derive the critical domain size and the minimal travelling wave speed.

We can rewrite Equation (17) in a more compact form as a nonlinear Fisher–KPP equation, namely

$$u_t = (D(u)u)_{xx} + f(u) \quad (18)$$

with

$$D(u) = d_K \alpha(u) + d_S \beta(u) \quad (19)$$

and $f(u)$ as defined in Equation (2). One immediate observation is the fact that, for general rates $\alpha(u)$ and $\beta(u)$, the above model can lead to negative diffusion, which is not well defined. To avoid this, we make a simple assumption.

Assumption A1 Assume that $D(u)$ satisfies

$$\inf_u \{D'(u)u + D(u)\} > 0. \quad (20)$$

With Assumption (A1), Equation (18) is uniformly parabolic [10] and standard solution theory can be applied. If Equation (18) is equipped with proper boundary conditions on a smooth spatial domain, then the corresponding initial-value problem has unique classical solutions. Since existence theory for equations of the type (18) is covered in the classical literature [24], we do not treat the details of the existence theory here.

3.1.2. The pure birth-jump case

An important special case arises if there is no spontaneous travel, i.e. $\alpha = 0$, and spatial spread is possible only by newly created individuals. In this case, Equation (1) describes a pure birth-jump process,

$$u_t = \int_{\Omega} S(x, y, u) \beta(u) u \, dy - \delta(u) u. \quad (21)$$

Equation (21) is closely related to well-known integro-differential spread models. In particular, if β is constant, and if we allow δ to include all population dynamics, i.e. $-\delta(u)u = g(u)$, where we relax the assumption that δ should be non-negative, then we obtain

$$u_t = \beta \int_{\Omega} S(x, y) u \, dy + g(u), \quad (22)$$

which has been studied extensively (see [14,19,20,26,40]). Note that Equation (22) assumes independence of spatial spread and reproduction. Our pure birth-jump process described by Equation (21) is significantly different as reproduction triggers spread. Nevertheless, many methods developed for Equation (22) can and will be used for the analysis of Equation (21).

The diffusion limit for Equation (21) is (compare with Equation (17))

$$u_t = d_S (\beta(u)u)_{xx} + (\beta(u) - \delta(u))u, \quad (23)$$

and Assumption (A1) then is an assumption on the growth rate, namely

$$\inf_u \{\beta'(u)u + \beta(u)\} > 0.$$

3.1.3. Examples

Here, we highlight three specific examples of well-known growth models.

(1) In the case of *logistic growth*, $f(u) = \mu u(1 - u/C)$, we can choose

$$\beta(u) = \mu \quad \text{and} \quad \delta(u) = \frac{\mu u}{C}$$

to satisfy Assumption (A1).

(2) For *Ricker growth*, $f(u) = \mu u e^{-\gamma u}$, we have to be a bit more careful. Each choice $\phi \geq 1$ with

$$\beta(u) = \mu(\phi + u) \quad \text{and} \quad \delta(u) = \mu(\phi + u - e^{-\gamma u})$$

leads to rates that satisfy Assumption (A1).

(3) Also, an *Allee effect* can be included in this framework. If the kinetic term has the form $f(u) = \mu u(1 - u)(u - \gamma)$ for $0 < \gamma < 1$, then a suitable choice is

$$\beta(u) = \mu(1 + \gamma)u \quad \text{and} \quad \delta(u) = \mu(\gamma + u^2).$$

3.2. Critical domain size problem

For the critical domain size problem, we are interested in finding the smallest domain able to sustain a stable population [39]. We study this problem for the nonlinear diffusion limit (17) on an interval $[0, L]$ with homogeneous Dirichlet boundary conditions $u(0, t) = 0$ and $u(L, t) = 0$. To find the critical domain size, we use two methods. In Section 3.2.1, we analyse the critical length $L_{\text{crit}}^{(1)}$ such that the homogeneous steady state $u \equiv 0$ becomes linearly unstable for $L > L_{\text{crit}}^{(1)}$. Second, in Section 3.2.2, we find the critical length $L_{\text{crit}}^{(2)}$ such that Equation (17) has a non-trivial steady-state solution. In the case of $D(u) = \text{const}$, it is well known that these two critical values coincide [39]. This is the case here too, and we show that

$$L_{\text{crit}}^{(1)} = L_{\text{crit}}^{(2)} = \pi \sqrt{\frac{D(0)}{f'(0)}} = \pi \sqrt{\frac{d_K \alpha(0) + d_S \beta(0)}{\beta(0) - \delta(0)}}. \quad (24)$$

In Section 3.2.3, we summarize the critical domain size results in the context of the pure birth-jump process (i.e. $\alpha = 0$) for the logistic growth model and the Ricker growth model, and we conclude with a numerical investigation of the critical domain size problem.

3.2.1. Critical domain size from linearization at zero

To develop the critical domain size, we work with the compact form of Equation (17), namely the nonlinear Fisher–KPP Equation (18). We rewrite Equation (18) as

$$u_t = (D''(u)u + 2D'(u))u_x^2 + (D'(u)u + D(u))u_{xx} + f(u),$$

and linearization at zero gives

$$u_t = D(0)u_{xx} + f'(0)u. \quad (25)$$

A Fourier transform leads to an eigenvalue problem

$$\lambda = -\omega^2 D(0) + f'(0),$$

where on $[0, L]$ with homogeneous Dirichlet boundary conditions we have the characteristic values of $\omega = n\pi/L$ for $n = 1, 2, \dots$. We are interested in the leading positive eigenvalue for

$n = 1$. The condition for the critical length $L_{\text{crit}}^{(1)}$ arises from the equality

$$-\frac{\pi^2}{(L_{\text{crit}}^{(1)})^2}D(0) + f'(0) = 0,$$

which gives

$$L_{\text{crit}}^{(1)} = \pi \sqrt{\frac{D(0)}{f'(0)}}.$$

For each $L > L_{\text{crit}}^{(1)}$, the linearization (25) has a positive eigenvalue, making $u \equiv 0$ linearly unstable. Substituting $D(u)$ as defined in Equation (19) and $f(u)$ as defined in Equation (2) leads to the critical domain size result (Equation (24)) stated above.

3.2.2. Critical domain size from existence of non-trivial steady states

To analyse the steady-state equation related to Equation (18), namely

$$(D(u)u)'' + f(u) = 0, \tag{26}$$

we introduce $v := (D(u)u)'$ to obtain the equivalent system

$$\begin{aligned} (D(u)u)' &= v, \\ v' &= -f(u). \end{aligned}$$

Since $(D(u)u)' = (D'(u)u + D(u))u'$ and $D'(u)u + D(u) > 0$ by assumption (A1), the system can be rewritten as

$$\begin{aligned} u' &= \frac{v}{D'(u)u + D(u)}, \\ v' &= -f(u). \end{aligned} \tag{27}$$

Using the solution of this system, $u(x)$, we define a monotonic transformation

$$\xi := \int_0^x (D'(u)u + D(u))^{-1}(y) dy. \tag{28}$$

Then,

$$\frac{d}{dx} = \frac{d\xi}{dx} \frac{d}{d\xi} = (D'(u)u + D(u))^{-1} \frac{d}{d\xi}$$

such that the transformed variables $w(\xi) = u(x)$, $z(\xi) = v(x)$ satisfy

$$\begin{aligned} w' &= z, \\ z' &= -f(w)(D'(w)w + D(w)). \end{aligned} \tag{29}$$

The dynamical systems (27) and (29) have the same orbits. Hence, whenever Equation (29) admits non-trivial solutions with homogeneous Dirichlet boundary conditions, then so does Equation (27). The only difference is the length of these solution, since the length parameter x has been rescaled.

As we analyse Equation (29), we recognize that this is the critical domain size problem for the reaction–diffusion equation with constant diffusion coefficient, i.e.

$$\begin{aligned} w_t &= w_{xx} + F(w), \\ F(w) &= f(w)(D'(w)w + D(w)). \end{aligned} \tag{30}$$

This model has been analysed many times [39], and it is known in this case that the critical domain size is

$$L_{\text{crit}}^\xi = \pi \sqrt{(F'(0))^{-1}} = \pi \sqrt{(D(0)f'(0))^{-1}}.$$

Equation (29) has non-trivial steady states for each $L > L_{\text{crit}}^\xi$. We use the superscript ξ to indicate that this length relates to the transformed space variable. To find a corresponding expression in the original variable x , we need to invert the relation

$$L_{\text{crit}}^\xi = \int_0^{L_{\text{crit}}^{(2)}} (D'(u)u + D(u))^{-1}(y) \, dy, \tag{31}$$

which is hard to do. However, close to the critical value, the solution u is close to zero, and we make the approximation

$$L_{\text{crit}}^\xi = \int_0^{L_{\text{crit}}^{(2)}} (D'(u)u + D(u))^{-1}(y) \, dy \approx \frac{1}{D(0)} \int_0^{L_{\text{crit}}^{(2)}} dy = \frac{L_{\text{crit}}^{(2)}}{D(0)},$$

from which we obtain

$$L_{\text{crit}}^{(2)} = D(0)L_{\text{crit}}^\xi = \pi \sqrt{\frac{D(0)}{f'(0)}}.$$

Note that even though we cannot completely invert the integral in Equation (31), we still know that the transformation $x \mapsto \xi$ is monotonic. Hence, non-homogeneous solutions of Equation (26) exist for all $L > L_{\text{crit}}^{(2)}$. We have found $L_{\text{crit}}^{(2)} = L_{\text{crit}}^{(1)}$ and the critical domain size result (24) stated above follows.

3.2.3. Examples

- (1) For the case of a pure birth-jump process ($\alpha = 0$) and logistic growth, we have $\beta(u) = \mu$ and $\delta(u) = \mu u/C$. Then, the critical domain size result (24) gives

$$L_{\text{crit}} = \pi \sqrt{d_S}.$$

Notice that this value does not depend on the growth rate μ , which is related to the fact that the growth rate μ appears in both the diffusion term and the kinetic term, and they cancel each other in the formula for L_{crit} .

- (2) For the case $\alpha = 0$ and Ricker growth, we have $\beta(u) = \mu(\phi + u)$ and $\delta(u) = \mu(\phi + u - e^{-\gamma u})$ with $\phi \geq 1$. In this case, the critical domain size result (24) gives

$$L_{\text{crit}} = \pi \sqrt{d_S \phi}.$$

Notice that the critical domain size explicitly depends on the free parameter ϕ , which shows that it is important to choose the birth and death rates $\beta(u)$ and $\delta(u)$ carefully.

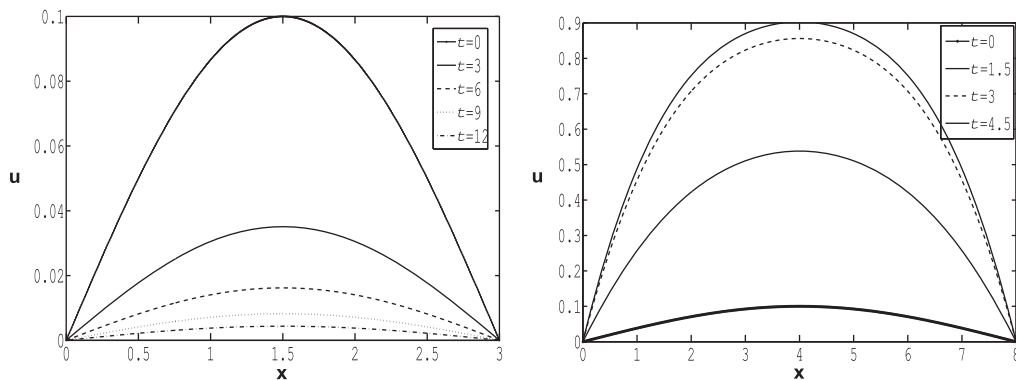


Figure 1. Illustration of the critical domain size problem. Numerical simulation of model (32) with $a = 1$, $\mu = 2$, and $C = 1$, for $L = 3$ (left) and $L = 8$ (right). On the left, the time shots for $t = 0, 3, 6, 9$, and 12 show a decaying solution; on the right, the time shots for $t = 0, 1.5, 3$, and 4.5 show a growing solution.

- (3) To numerically illustrate our critical domain size result, we consider the logistic growth model with

$$d_K = d_S = 1, \quad \alpha(u) = \frac{u}{a+u}, \quad \beta(u) = \mu, \quad \delta(u) = \frac{\mu u}{C},$$

where the free parameters a , μ , and C are all assumed to be positive. We choose a monotonically increasing, saturating shedding rate α , which implies that we expect that shedding does not increase unboundedly with density. Inserting these forms into Equation (17), we obtain

$$u_t = \left(\left(\mu + \frac{u}{a+u} \right) u \right)_{xx} + \mu \left(1 - \frac{u}{C} \right) u. \quad (32)$$

Here, $D(u) = \mu + u/(a+u)$ and $f(u) = \mu u(1 - u/C)$, so our result (24) implies that the critical domain size in this case is

$$L_{\text{crit}} = \pi.$$

We use the software package FlexPDE to solve this nonlinear equation for parameter values $a = 1$, $\mu = 2$, and $C = 1$. FlexPDE employs a finite-element, Newton–Raphson method to numerically solve the Dirichlet initial-boundary value problem for Equation (32) [32]. The spatio-temporal mesh is adaptively refined at each time step to control numerical error. We assume that the population is non-zero initially and smoothly varies throughout the entire domain. We model this by the initial condition

$$u(x, 0) = 0.1 \left(\sin \frac{\pi x}{L} \right). \quad (33)$$

In Figure 1, we show solutions for two values of L , namely one subcritical ($L = 3$) and one supercritical ($L = 8$). For the domain size $L = 3$, the solution decays to zero, while for $L = 8$, the solution grows to a stationary distribution. We simulated many more parameter choices, and the critical length L_{crit} result was confirmed in each case (results not shown).

3.3. Travelling wave problem

Travelling waves for the diffusion limit (17) are self-similar solutions of the form $u(x - ct)$, where c denotes the invasion speed. We determine the minimal wave speed for this equation in Section 3.3.1, and we discuss examples in Section 3.3.2.

3.3.1. Minimal wave speed

To develop the minimal wave speed, we again work with Equation (18), the compact form of the nonlinear Fisher–KPP equation (17). If we substitute $u(x - ct)$ into Equation (18), then we obtain

$$-cu' = (D(u)u)'' + f(u),$$

where the prime denotes differentiation with respect to $\eta = x - ct$. We introduce $v := (D(u)u)'$ and obtain the system

$$\begin{aligned} (D(u)u)' &= v, \\ v' &= -cu' - f(u). \end{aligned}$$

We have $v = (D(u)u)' = (D'(u)u + D(u))u'$, where $D'(u)u + D(u) > 0$, by Assumption (A1), so that the above system can be rewritten as

$$\begin{aligned} u' &= \frac{v}{D'u + D}, \\ v' &= -\frac{cv}{D'u + D} - f(u). \end{aligned}$$

As in the preceding subsection, we use a spatial rescaling of the system (see Equations (28) and (30)): we multiply both equations by a common positive factor $D'u + D$, which leaves the orbits invariant. Hence, we study the orbits of

$$\begin{aligned} w_t &= z, \\ z_t &= -cw - f(w)(D'(w)w + D(w)). \end{aligned}$$

We recognize that this system is the travelling wave system corresponding to Equation (30). The travelling wave problem for this equation has been solved many times [8,10,36]. Before we can apply the general results for this equation to our situation, we need to ensure that the new nonlinearity $F(w) = f(w)(D'(w)w + D(w))$ is monostable and satisfies linear determinacy. This means

- (1) *monostability*: $F(0) = 0$, $F'(0) > 0$, $F(\bar{w}) = 0$, and $F(w) > 0$ for all $w \in (0, \bar{w})$, where $\bar{w} = \infty$ is possible.
- (2) *linear determinacy*: $F'(w) \leq F'(0)w$ for all $w \in (0, \bar{w})$.

THEOREM 3.1 *Assume (A1) and assume that $f(u) = (\beta(u) - \delta(u))u$ is monostable, then $F(u)$ also is monostable. If, in addition, $F(u)$ is linearly determined, then there exists a minimal wave speed of Equation (17) given by*

$$c^* = 2\sqrt{D(0)(\beta(0) - \delta(0))} = 2\sqrt{(d_K\alpha(0) + d_S\beta(0))(\beta(0) - \delta(0))}. \quad (34)$$

Initial conditions with compact support will approximate, two waves traveling left and right with speed c^ and $-c^*$, respectively. Moreover, for each $c > c^*$ there exists a self-similar solution with speed c .*

Proof We apply the results of [8] to Equation (30). Given the above assumptions, the minimal wave speed for Equation (30) is

$$c^* = 2\sqrt{F'(0)} = 2\sqrt{f'(0)D(0) + 2f(0)D'(0)}.$$

Using $f(u)$ as defined in Equation (2), we have $f(0) = 0$ and $f'(0) = \beta(0) - \delta(0)$, and the minimal wave speed result for Equation (17) follows. ■

3.3.2. Examples

- (1) For the case of a pure birth-jump process ($\alpha = 0$) and logistic growth, we have $\beta(u) = \mu$ and $\delta(u) = \mu u/C$. Then, $F(u) = \mu^2 d_S u(1 - u/C)$, which is clearly monostable and linearly determined. In this case, the minimal wave speed (Equation (34)) is

$$c^* = 2\sqrt{d_S \mu^2}.$$

- (2) For the case $\alpha = 0$ and Ricker growth, we have $\beta(u) = \mu(\phi + u)$ and $\delta(u) = \mu(\phi + u - e^{-\gamma u})$ with $\phi \geq 1$. Then, $F(u)$ is given by

$$F(u) = \mu^2 d_S u^2 \phi e^{-\gamma u}.$$

In this case, $F'(0) = 0$, and $F(u)$ is not linearly determined as assumed above. Hence, the above theorem does not apply to this case.

- (3) To numerically illustrate the travelling wave solution, we again use example (Equation ((32))). In this case, $\alpha(0) = 0$, $d_S = 1$, $\beta(0) = \mu$, and $\delta(0) = 0$, so that our result (Equation ((34))) implies that the minimal wave speed is

$$c^* = 2\mu. \quad (35)$$

We use FlexPDE [32] to solve Equation (32) on the domain $[0, L]$ with homogeneous Neumann boundary conditions. We again use parameter values $a = 1$, $\mu = 2$, and $C = 1$ and set $L = 100$. The initial condition u_0 , given by

$$u_0(x) = \exp\left(-\frac{x^2}{0.01}\right), \quad (36)$$

concentrates the initial mass near zero. The solution then develops into a travelling wave until it reaches the boundary at L . In Figure 2, we show the wave profile at various times. We observe a wave speed of $c^* = 4$, as predicted by Equation (35). We tried several other combinations of parameters, and all confirm the minimal wave speed to be given by Equation (35) (results not shown).

4. Application to fire spotting

Birth-jump models have been used in several applications, and we discuss a few of them in the discussion section. In this section, we apply the birth-jump process to the phenomenon of forest fire spotting. In Section 4.1, we give an introduction to forest fire spotting. In Section 4.2, we use the birth-jump framework to develop the spotting model. In Section 4.3, we apply the results from Section 3, and determine the critical domain size and invasion speed of a forest fire. We show that spotting can substantially increase the rate of spread of a fire invasion front.

4.1. Introduction to forest fire spotting

Wildfire is an essential phenomenon for many terrestrial ecosystems.² Wildfires are typically classified as surface, ground or canopy (crown) fires, the latter being the most intense. In the Boreal forest, crown fires leave few trees standing in their wake; the carbon-rich environment left behind is prime real-estate for the establishment of new plants, as in the case of aspen or

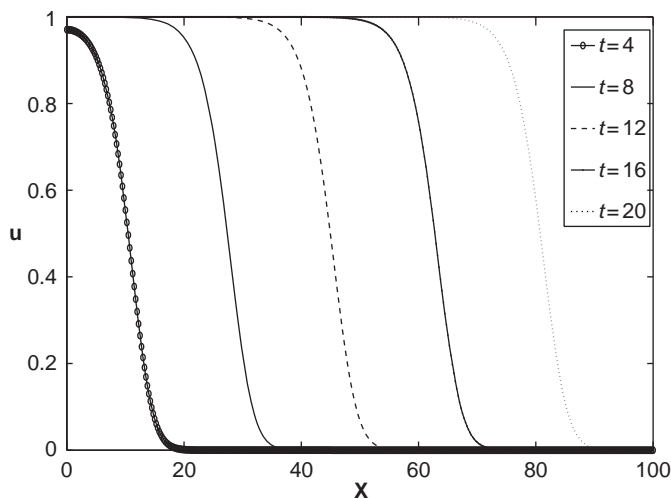


Figure 2. Illustration of the travelling wave problem. Travelling wave profile for Equation (32) at times $t = 4, 8, 12, 16,$ and 20 , from left to right. Parameter values are $a = 1, \mu = 2,$ and $c = 1,$ and the domain length is $L = 100.$ The minimal wave speed is $c^* = 4.$

lodgepole pine. Wildfires become dangerous when they occur in the wildland–urban interface, as they may cause serious damage to human developments like industry or property. Due to the ever-expanding radius of human activity, fire management operations must be as well informed as possible – in turn, this further mandates an improvement of our fundamental understanding of wildfire behaviour.

Much empirical data have been collected for local wildfire spread [12]. The most important metric is the rate of spread, which characterizes how fast a wildfire front will expand with time in the direction normal to itself. Regression analysis of field data, for a variety of spread scenarios, provides the rate of spread as a function of fuel type and distribution, topography, and weather. Because of the enormous variety of grassland, shrub, or forest stand types, which vary in character across the globe, many empirically based systems have been developed to predict wildfire front evolutions for fire management [5,11,12,38].

Despite these developments, there remain several aspects of wildfire behaviour that are poorly understood. Of particular importance for fire management is wildfire spotting (or simply spotting). Spotting describes the launch of burning material into the wind column, its transport ahead of the fire, its landing, and the subsequent ignition of a new fire (a spot fire) [1,2,15,22]. Spotting distances are often quite short (several metres), but in many cases long-distance spotting is also observed (up to several kilometres). Spotting is the most common cause for the escape of prescribed fires. Spot fires can cause breaches across roads, rivers or regions which might otherwise slow local spread, perhaps placing valuable assets in unexpected danger. Spot fires also may be responsible for increased rates of spread or acceleration of fronts.

4.2. Development of the spotting model

Since spotting is an important factor of fire spread, many of its sub-processes (firebrand generation, launching in the convection column, downwind transport, combustion, terminal falling velocity, and fuel bed ignition) have received detailed scientific attention. It is impossible, in this paper, to explain the complete physical processes, hence we will only present and discuss the resulting fire spotting model from [28]. We refer to [28] for details on the underlying physical

combustion laws. Our fire spotting model is based on the idea of a *spotting distribution*, which was formulated for the first time in [28,29].

The birth-jump framework is naturally suited to model forest fire spotting. Indeed, burning firebrands are ‘shed’ from the main fire into the atmosphere and subsequently ‘settle’ downwind to possibly start a new fire. To relate our general model (1) to forest fire spread, we imagine a long fire front spreading in the y direction. The probability of having no fire at location x before a time T is assumed to be governed by a Poisson process, such that the cumulative probability P satisfies

$$P(\text{no fire at } x \text{ before } T) = \exp\left(-\int_0^T u(x, t) dt\right),$$

where $u(x, t)$ is the expected instantaneous fire probability at location x at time t . In what follows, we focus on deriving a model for $u(x, t)$. We consider the fire expectation $u(x, t)$ to be influenced by three processes: (i) local spread, (ii) spotting, (iii) combustion and extinction. We assume our medium to be homogeneous and flat, as in the case of an extended, dense coniferous forest.

The first two terms on the right-hand side of Equation (1) are used to describe local fire spread. We assume a constant spread rate $\alpha = \text{const}$, and we assume that the kernel K is locally concentrated. Hence, as done before, this term becomes a standard diffusion term. Many other fire spread models use diffusion for local spread as well [4,5]. Fire does tend to spread faster in the wind direction, which might motivate an anisotropic diffusion term, but we assume that spotting is more affected by wind, and local spread not so much, hence standard diffusion is sufficient to describe local spread.

The spotting process is described by the birth-jump term in Equation (1). The kernel S now has the meaning of a spotting kernel [28,29], i.e. $S(x, y, u(x, t))\Delta x$ is the probability that a fire at location y creates a spot fire in $[x, x + \Delta x]$ during the time interval $[t, t + \Delta t]$. Implicit in this definition is the assumption that spotting is instantaneous, i.e. the flight time of burning firebrands is short (minutes) compared to the overall fire progression (hours or days). In [28], it is shown how the model can be extended if the flight time, or the time to crowning, needs to be accounted for. This leads to a time delay in the spotting term. The spotting kernel S depends on the expected fire probability $u(x, t)$ at the landing site x . When a fire is already burning at x , then spotting will not much increase the fire probability. In [28], physical principles have been used to find explicit forms for the spotting kernel S . We present some of them with our numerical simulations later.

The last term in Equation (1) is used to describe combustion and extinction. At this point, we need to introduce a new variable $v(x, t)$ for the total fuel loading density (a measure of how much fuel is available for combustion). Our first forest fire spread model for a fire front that advances in the x direction is given by

$$\begin{aligned} u_t &= Du_{xx} + \int_{-\infty}^{\infty} S(x, y, u(x, t))u(y, t) dy + \gamma\tilde{c}(u, v)v - \delta(u)u, \\ v_t &= -\tilde{c}(u, v)v. \end{aligned} \tag{37}$$

The term $\tilde{c}(u, v)$ is the combustion rate and the factor γ converts fuel into fire probability.

An important case arises if we assume that fuel consumption is relatively slow such that $v \approx \text{const}$. Then, system (37) reduces to

$$u_t = Du_{xx} + \int_{-\infty}^{\infty} S(x, y, u(x, t))u(y, t) dy + c(u)u - \delta(u)u, \tag{38}$$

with $c = \gamma\tilde{c}$. When the spotting kernel S is symmetric, we call Equation (38) as the *no-wind spotting equation*.

If the wind is blowing in the x direction, then we can assume that burning embers fly downwind and spotting occurs in the positive x direction only. In this case, the spotting kernel $S(x, y, u)$ will only depend on burning locations y that are to the left of x , resulting in

$$u_t = Du_{xx} + \int_{-\infty}^x S(x, y, u(x, t))u(y, t) dy + c(u)u - \delta(u)u. \tag{39}$$

We call Equation (39) as the *constant-wind spotting equation*.

4.3. Critical domain size and invasion speed

In this section, we use the theory developed in Section 3 to estimate the critical domain size and the minimal invasion speed for the spotting models and to determine their dependence on the spotting kernel S . We do this in two steps. In Section 4.3.1, we consider the no-wind spotting equation (38). In Section 4.3.2, we consider the constant-wind spotting equation (39). In this case, the integral term is no longer symmetric, and an additional drift term arises. We show numerical simulations to support the theoretical results; as in Section 3, we use FlexPDE to generate our numerical results [32].

For the numerical simulations, we choose a logistic birth term $c(u)u = \mu u(1 - u/C)$, with constant per-capita heat loss $\delta = d > 0$. These and other forms of the combustion and heat-loss terms have been analysed in [28], where some models could be derived from regression analysis of field data (see, e.g. [12]). Our choice above is a typical representation of these models. It is a goal of future research to determine quantitatively more accurate functional forms for $c(u)u$ and $\delta(u)u$, in the context of models (38) and (40).

4.3.1. No wind case

In this section, we consider the no-wind spotting Equation (38) and assume that the spotting kernel S is symmetric with zero- and second-moments given as

$$\sigma(x, u) = \int_{-\infty}^{\infty} S(x, y, u) dy, \quad d_s(x, u) = \int_{-\infty}^{\infty} \frac{(y - x)^2}{2} S(x, y, u) dy.$$

We assume that the medium is homogeneous, such that the moments of S are the same at each location, and we assume that the spotting intensity σ is constant, i.e.

$$\sigma = \text{const.} \quad d_s = d_s(u).$$

Using the moment expansion from Section 3, we obtain the following parabolic equation to second order:

$$u_t = ((D + d_s(u))u)_{xx} + (\sigma + c(u) - \delta(u))u. \tag{40}$$

This equation is of the form of Equation (17), and so we can directly apply our general results for the critical domain size Equation (24) and for the minimal invasion speed Equation (34).

LEMMA 4.1 *Assume that $\sigma = \text{const.}$, and $d_s(u)$ satisfies $d'_s(u)u + D + d_s(u) > 0$ and that $f(u) = (\sigma + c(u) - \delta(u))u$ is monostable. Then, the critical domain size is given by*

$$L_{\text{crit}} = \pi \sqrt{\frac{D + d_s(0)}{\sigma + c(0) - \delta(0)}} \tag{41}$$

and the minimum invasion speed is

$$c^* = 2\sqrt{(D + d_s(0))(\sigma + c(0) - \delta(0))}. \tag{42}$$

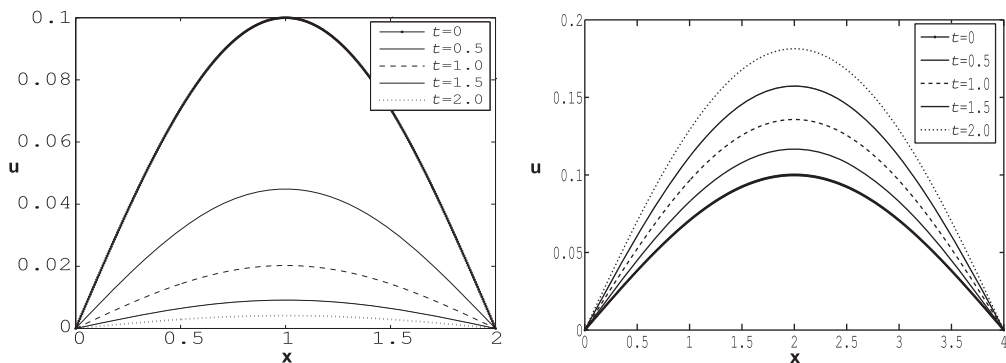


Figure 3. Illustration of the critical domain size problem for Equation (40), with $D = 1$, $\mu = 0.5$, $C = 1$, $\sigma = 1$, and $l = 0.5$, for which $L_{\text{crit}} = 3.2$. Starting from the initial condition given in Equation (33), numerical simulations are shown for $L = 2$ (left) and $L = 4$ (right). In the left image, the time shots for $t = 0, 0.5, 1, 1.5$, and 2 show a decaying solution; in the right image, time shots indicate a growing solution.

The two spotting parameters are the spotting intensity or spotting rate σ and the spotting spread (or variance) d_s . We observe that a larger spotting rate σ reduces the critical domain size. That is, a fire which shows more spotting can be sustained in a smaller environment. At the same time, a larger spotting spread at 0, $d_s(0)$, increases the critical domain size, as one would expect intuitively. Further, we observe that a larger spotting rate σ and a larger spotting spread $d_s(0)$ both increase the minimum invasion speed. Based on our model, spotting thus increases the invasion speed of a wildfire front.

For numerical illustration, we consider the example of a homogeneous environment, where the spotting kernel is both independent of the density u and symmetric. In reality, all spotting kernels S have compact support, since there is a finite time-horizon beyond which embers have already burned out before landing, and no spot fires result. The specific example used below is a symmetric uniform kernel $S = S_1(-l, l)(y)$, where S_1 is $\sigma/2l$ when $y \in [-l, l]$ and zero otherwise; notice that this kernel is not necessarily normalized.

To validate our critical domain size result ((Equation (41))), we compute the second moment d_s of the uniform kernel. Since the kernel does not depend on space, we can determine the second moment by integrating about 0. In terms of the parameter l , which measures the spatial extent of the spotting effect, we find

$$d_s = \int_{-l}^l \frac{\sigma}{2l} \frac{y^2}{2} dy = \frac{\sigma l^2}{6}. \quad (43)$$

In Figure 3, we show the solutions of Equation (40) with homogeneous Dirichlet boundary conditions on $[0, L]$ with $D = 1$, $\mu = 0.5$, $C = 1$, $\sigma = 1$, and $l = 0.5$. Employing the preceding expression for d_s in the critical domain size formula (41), we expect the critical domain size to be approximately $L_{\text{crit}} = 3.2$. This result is confirmed in Figure 3, where we show both a subcritical case for the domain size ($L = 2.0$) as well as a supercritical case ($L = 4.0$). As expected, for the sinusoidal initial conditions given in Equation (33), we observe a decaying solution when $L = 2.0$, and a growing solution when $L = 4.0$. We tested many more parameter values (not shown), which all confirmed the theoretical formula (41).

Next, we validate the travelling wave spreading speed formula (42). We again use parameter values $D = 1$, $\mu = 0.5$, $C = 1$, and $\sigma = 1$, and choose a symmetric uniform spotting kernel with parameter $l = 0.5$. Starting from a half-Gaussian initial condition of the form (36), once the solution has reached its equilibrium shape and rate of spread, we keep track of the level set $\{u(x, t) = 0.3\} := x_f(t)$ over time. By comparing $x_f(t)$ at two values $t_1 < t_2$, we can approximate the spreading speed by the difference $(x_f(t_2) - x_f(t_1))/(t_2 - t_1)$. Again we checked the validity

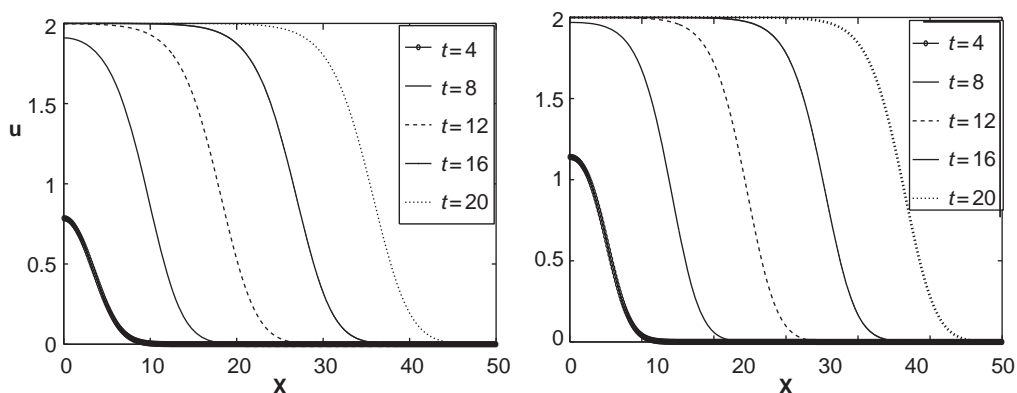


Figure 4. Illustration of the travelling wave problem for Equation (40) without wind (left) and Equation (45) with wind (right). (Left) Travelling wave profile for Equation (40) at times $t = 4, 8, 12, 16,$ and 20 , from left to right. Parameter values are $D = 1, \mu = 0.5, C = 1,$ and $\sigma = 1$; the spotting kernel is symmetric and uniform with parameter $l = 0.5$, and the domain length is $L = 50$. The asymptotic spreading speed is $c^* \approx 2.04$. (Right) Travelling wave profile for Equation (45) at times $t = 4, 8, 12, 16,$ and 20 , from left to right. Parameter values are $D = 1, \mu = 0.5, C = 1,$ and $\sigma = 1$; the spotting kernel is one-sided and uniform with parameter $l = 0.5$, and the domain length is $L = 60$. The asymptotic spreading speed is $c^* \approx 2.54$, which is clearly faster than the no-wind case illustrated on the left, where we have employed identical parameters, but a symmetric uniform spotting kernel.

of Equation (42) for a variety of parameter choices (not shown). For our choice of parameters, we expect a speed of $c^* \approx 2.04$. This speed is confirmed in Figure 4 (left), where we show snapshots in time of our solution over a spatial domain of (unitless) length 50.

4.3.2. Constant-wind case

In this section, we consider the constant-wind spotting equation (Equation (39)). The integral no longer is symmetric, and we need to adapt the definitions of our moments accordingly:

$$\begin{aligned} \sigma(x, u) &:= \int_{-\infty}^x S(x, y, u) \, dy, \\ \nu(x, u) &:= - \int_{-\infty}^x (y - x) S(x, y, u) \, dy, \\ d_s(x, u) &:= \int_{-\infty}^x \frac{(y - x)^2}{2} S(x, y, u) \, dy. \end{aligned}$$

For convenience, we introduce a minus sign for the first moment, such that positive ν leads to drift in the positive x direction. Even if we assume that the spotting kernel is identical at each location, these moments still depend on x , since the integral boundary depends on x . However, if S has compact support, as is often the case, and if x is large enough, then the moments are constant. Hence, we assume that S has compact support and x is large enough such that $[-\infty, x]$ covers the support of S . This assumption implies that we cannot apply our theory from Section 3 to determine the critical domain size (since small x are considered). But we can use it for the invasion speed, since large x are of interest. The first moment ν describes the influence of the wind. It has dimensions of a velocity, but it is not the wind velocity; rather, it describes the net drift on burning embers due to flight in wind. We assume this net drift is constant.

Using this assumption combined with the previous assumptions, we consider

$$\sigma = \text{const.}, \quad \nu = \text{const.}, \quad d_s = d_s(u). \tag{44}$$

In this case, Equation (40) becomes

$$u_t + (vu)_x = ((D + d_s(u))u)_{xx} + (\sigma + c(u) - \delta(u))u. \quad (45)$$

We change to moving coordinates $U(x, t) := u(x - vt, t)$ and obtain

$$U_t = ((D + d_s(U))U)_{xx} + (\sigma + c(U) - \delta(U))U, \quad (46)$$

which is identical to Equation (40). The results from Lemma 4.1 apply to $U(x, t)$. If we transform back to $u(x, t)$, we obtain the following result:

LEMMA 4.2 *Assume S has compact support and x is larger than the support of S . Further assume that $\sigma = \text{const.}$, $v = \text{const.}$, and $d_s(u)$ satisfies $d'_s(u)u + D + d_s(u) > 0$ and that $f(u) = (\sigma + c(u) - \delta(u))u$ is monostable. Then, the minimum invasion speed is*

$$c^* = 2\sqrt{(D + d_s(0))(\sigma + c(0) - \delta(0))} + v. \quad (47)$$

To illustrate the wave formula (47) numerically, we again assume that spread occurs in a homogeneous medium, and choose parameters $D = 1$, $\mu = 0.5$, and $C = 1$. We will again work with a uniform spotting kernel, which we will write $S = S_2(-l, 0)(y)$, where l is a parameter which measures the extent upwind from which firebrands may reach us at location y . To be precise, $S_2(-l, 0)(y) = \gamma/l$ for $y \in [-l, 0]$ and zero otherwise. Before simulating Equation (39), we compute the moments of S as

$$\begin{aligned} \sigma &= \int_{-l}^0 \frac{\gamma}{l} dy = \gamma, \\ v &= \int_{-l}^0 -\frac{\gamma y}{l} dy = \frac{\gamma l}{2}, \\ d_s &= \int_{-l}^0 \frac{\gamma y^2}{2l} dy = \frac{\gamma l^2}{6}. \end{aligned}$$

We assume here $\gamma = 1$ so that $\sigma = 1$, as in the no-wind case from the preceding subsection, and again choose $l = 0.5$.

According to Equation (47), we expect the asymptotic spreading speed to increase from 2.04 to $c^* \approx 2.54$. This speed is confirmed in Figure 4 (right), where we see that the solution wave travels with the appropriately increased speed relative to the waves displayed in Figure 4 (left). Our spreading speed formula was validated for a variety of other model parameters (results not shown).

5. Discussion

Birth-jump processes apply to situations in which growth and spatial spread are coupled, for example when newly generated individuals undergo immediate translocation. Birth-jump models thus are a distinct class of models, separate from standard reaction–diffusion models (for which growth and spatial spread are assumed to be independent processes).

Birth-jump models take the form of nonlinear integro-differential equations. In the case where the integral terms are linear, a sophisticated theory has been developed, which includes existence and uniqueness of solutions, stabilities, and travelling waves [14,19,20,27,40].

The theory for nonlinear birth-jump processes is just beginning and first theoretical results are in preparation [7].

In this paper, we have presented two derivations of the general birth-jump integro-differential equation. Further, we have shown that, when the redistribution kernels K and S are highly concentrated, the integro-differential equation can be approximated by a generalized reaction–diffusion equation (Equation (17)). It is important to note that in this generalized reaction–diffusion equation, the proliferation rate contributes to both the diffusion term and the reaction term. We have fully solved the critical domain size problem and the minimal wave speed problem for the resulting diffusion limit, obtaining expressions for the critical domain size (Equation (24)), and the minimal wave speed (Equation ((34))).

One interesting theoretical result presented here is the condition specified in Assumption (A1), namely that the rates α and β must be of a certain admissible form to ensure that the generalized reaction–diffusion equation is well defined. This might not be always the case. For example, for $\alpha = 0$, it is easily conceivable that $\beta(u)$ is a decreasing function of the population density, and hence Assumption (A1) might be violated. In that case, we have to include the next higher order approximation, which is a fourth-order term in Equation (14). If we keep this term, then (for $\alpha = 0$) we obtain instead of Equation (23) the limit equation

$$u_t = M_2(\beta(u)u)_{xx} + M_4(\beta(u)u)_{xxxx} + (M_0\beta(u) - \delta(u))u.$$

The fourth-order term regularizes if the coefficient in front of u_{xxxx} is negative. Here, the leading order coefficient is $(\beta'(u)u + \beta(u))u_{xxxx}$. Fourth-order terms are well known from the study of Cahn–Hilliard problems [3]: if the coefficient is negative, then this term regularizes and even controls the negative diffusion term. It is interesting to note that the second- and fourth-order terms have the same coefficient $\beta'u + \beta$. The condition for a positive diffusion coefficient is equivalent to the condition for a positive fourth-order coefficient. This means that for small values of u , the diffusion is proper and the fourth-order term is not needed, while for larger values of u , i.e. when $\beta'u + \beta < 0$, the fourth-order term regularizes and dominates the second-order term. It is an interesting open mathematical question to determine whether it is possible to construct a well-defined equation which only uses the fourth-order term in cases where the diffusion term has the wrong sign. If this were established, then Assumption (A1) could be relaxed.

Birth-jump processes show a great potential for mathematical modelling in biology, ecology, and medicine. In this paper, we have used the birth-jump approach to study applications to wild-fire spotting. We have developed two equations to describe the spread of a forest fire by spotting, namely a no-wind spotting equation and a constant-wind spotting equation. We have shown how spotting-driven fronts may travel faster than corresponding fronts which spread only locally by diffusion. In [28], more realistic models for kinetics and the spotting distribution are explored in detail. In [29], a mathematical framework for predicting spot fire distributions based on physical properties of flying and burning particles is developed. Future work includes exploring applications of the spotting distribution to wildfire breaching and rate of spread calculations.

In the context of ecology, we note a connection to the concept of the *IFD* of species. The IFD was introduced by Fretwell and Lucas in 1970 [13] to describe the observation that ‘Species distribute themselves such that fitness of each individual is the same’. It is quite normal to find many individuals at location of food availability and shelter, and fewer in bare areas. The fitness is a measure of reproductive success, which, in turn, correlates to availability of food and shelter. There is often a monotonic relationship between species distribution and fitness. If, for example, $m(x)$ denotes the fitness at location x and $\bar{u}(x)$ denotes the steady-state distribution of the population, then the IFD assumes that these are proportional [9,23], i.e.

$$\bar{u}(x) \sim m(x). \quad (48)$$

Our birth-jump process very naturally leads to the IFD. We assume that the two integral kernels K and S are identical, and that they depend only on the target location x , i.e.

$$K(x, y, u) = S(x, y, u) = K(x),$$

where we keep the symbol K for convenience. We assume that $K(x)$ is proportional to the fitness $m(x)$, i.e. $K(x) = vm(x)$, meaning that individuals prefer to settle at favourable locations. At steady state, the birth-jump model (1) becomes

$$(\alpha(\bar{u}(x)) + \delta(\bar{u}(x)))\bar{u}(x) = K(x) \int_{\Omega} (\alpha(\bar{u}(y)) + \beta(\bar{u}(y)))\bar{u}(y) dy. \quad (49)$$

The integral term on the right-hand side is independent of location x , and we call this constant J . If we further assume that the shedding rate α and the death rate δ are non-negative constants with $\alpha + \delta > 0$, then the steady state becomes

$$\bar{u}(x) = \frac{vJ}{\alpha + \delta} m(x),$$

and the population satisfies the IFD.

More generally, we can assume that $\alpha(u)$ and $\delta(u)$ are monotonic and non-decreasing in u . Then, also $h(u) = (\alpha(u) + \delta(u))u$ is monotonically increasing and has a monotonic inverse h^{-1} . The steady state \bar{u} is then a monotonic transformation of the fitness:

$$\bar{u}(x) = h^{-1}(vJm(x)).$$

Such a monotonic relationship might be a useful extension for the IFD, since it is less restrictive as the linear dependency. We suggest to call it a *weak IFD*, whereby it remains to be seen if this notion is useful in an ecological context.

It is noteworthy to observe that the IFD arises from the assumption that the redistribution depends on the target site only. A similar observation arises in [33], where a systematic study of different random walks is presented. The authors study random walks where the transitional probabilities depend on the target site, the release site, or some intermediate points. In their context, the IFD is relevant for random walks that depend on the target site, not on the point of release, similar to what we describe here.

The use of birth-jump processes also promises to be applicable in cancer modelling. In [17], Hillen *et al.* used a birth-jump process to describe the evolution of two cancer cell populations, namely cancer stem cells (cells with unlimited proliferative potential) and their non-stem cell descendants. They were able to show that the model supports the tumour growth paradox, which refers to the observation that a tumour, after incomplete treatment, may regrow to a larger size than it was before treatment.

Reaction–diffusion equations have shown their usefulness in many applications [30] and a rich qualitative theory is available [36]. However, they have limitations. Birth-jump processes allow us to access new areas of modelling, and we expect that they provide an equally rich menu for analysis and application.

Acknowledgements

Birth-jump processes developed out of an undergraduate research project of Robert Barrington-Leigh on ovarian cancer spread. Robert passed away at a young age and we dedicate this paper to him.

Notes

1. The development of the model is based on [6], and the derivations and the diffusion limit were developed in the Diplom thesis of BG [16] under the supervision of TH and GdeV.
2. We summarize some basic features of wildfires based on the textbooks of Johnson and Miyanishi [21], Pyne *et al.* [34], and Quintiere [35].

References

- [1] F.A. Albini, *Spot fire distance from burning trees – a predictive model*, Technical Report, Intermountain Forest and Range Experiment Station, Ogden, Utah, USDA For. Serv. Gen. Tech. Rep. INT-56, 1979.
- [2] F.A. Albini, *Transport of firebrands by line thermals*, Combust. Sci. Technol. 32 (1983), pp. 277–288.
- [3] N. Alikakos, P.W. Bates, and P. Fusco, *Slow motion for the Cahn–Hilliard equation in one space dimension*, J. Differential Equations 90 (1991), pp. 81–135.
- [4] P. Babak, A. Bourlioux, and T. Hillen, *The effect of wind on the speed of propagation of an idealized forest fire*, SIAM J. Appl. Math. 70(4) (2009), pp. 1364–1388.
- [5] J. Barber, C. Bose, A. Bourlioux, J. Braun, E. Brunelle, T. Garcia, T. Hillen, and B. Ong, *Burning issues with PROMETHEUS, the Canada’s wildfire growth simulator*, Can. Appl. Math. Q. 16(4) (2008), pp. 337–378.
- [6] R. Barrington-Leigh, G. de Vries, and T. Hillen, *Mathematical modelling of intraperitoneal cancer spread and radioimmunotherapy*, 2004, unpublished.
- [7] I. Borsi, A. Fasano, M. Primicerio, and T. Hillen, *Mathematical properties of a non-local integro-PDE model for cancer stem cells*, 2014, in preparation.
- [8] N.F. Britton, *Reaction–Diffusion Equations and their Applications to Biology*, Academic Press, London, 1986.
- [9] R.S. Cantrell, C. Cosner, and Y. Lou, *Approximating the ideal free distribution via reaction–diffusion–advection equations*, J. Differential Equations 245 (2008), pp. 3687–3703.
- [10] L.C. Evans, *Partial Differential Equations*, AMS Press, Providence, RI, 1998.
- [11] M.A. Finney, *FARSITE: Fire area simulator – model development and evaluation*, Technical report, USDA Forest Service, 2004.
- [12] Forestry Canada Danger Group, *Development and structure of the Canadian forest fire behaviour prediction system*, Technical report, Forestry Canada, 1992.
- [13] S.D. Fretwell and H.L. Lucas, *On territorial behavior and other factors influencing habitat distribution in birds I: Theoretical development*, Acta Biotheoretica 19 (1969), pp. 16–36.
- [14] J. Garnier, *Accelerating solutions in integro-differential equations*, SIAM J. Math. Anal. 43(4) (2011), pp. 1955–1974.
- [15] A. Gentaume, C. Lampin-Maillet, M. Guijarro, C. Hernando, M. Jappiot, T. Fonturbel, P. Perez-Gorostiaga, and J. Vega, *Spot fires: Fuel ammability and capability of firebrands to ignite fuel beds*, Int. J. Wildland Fire 18 (2009), pp. 951–969.
- [16] B. Greese, *Development, analysis and application of a nonlinear integro-differential equation in the context of cancer growth*, Diplomarbeit (MSc thesis), University of Greifswald, Germany, and University of Alberta, Canada, 2006.
- [17] T. Hillen, H. Enderling, and P. Hahnfeldt, *The tumor growth paradox and immune system-mediated selection for cancer stem cells*, Bull. Math. Biol. 75(1) (2013), pp. 161–184.
- [18] V. Hutson, S. Martinez, K. Mischaikow, and G.T. Vickers, *The evolution of dispersal*, J. Math. Biol. 47 (2003), pp. 483–517.
- [19] Y. Jin and M.A. Lewis, *Seasonal influences on population spread and persistence in streams: Spreading speeds*, J. Math. Biol. 65(3) (2011), pp. 403–439.
- [20] Y. Jin and M.A. Lewis, *Seasonal influences on population spread and persistence in streams II: Critical domain size*, SIAM J. Appl. Math. 71(4) (2011), pp. 1241–1262.
- [21] E.A. Johnson and K. Miyanishi, *Forest Fires*, Academic Press, San Diego, CA, 2001.
- [22] E. Koo, P.J. Pagni, D.R. Weise, and J.P. Woycheese, *Firebrands and spotting ignition in large-scale fires*, Int. J. Wildland Fire 19 (2010), pp. 818–843.
- [23] V. Krivan, R. Cressman, and C. Schneider, *The ideal free distribution: A review and synthesis of a game-theoretic perspective*, Theor. Popul. Biol. 73 (2008), pp. 403–425.
- [24] G.M. Lieberman, *Second Order Parabolic Differential Equations*, World Scientific, Singapore, 1996.
- [25] F. Lutscher, *Density-dependent dispersal in integrodifference equations*, J. Math. Biol. 56(4) (2007), pp. 499–524.
- [26] F. Lutscher, *A short note on short dispersal events*, Bull. Math. Biol. 69 (2007), pp. 1615–1630.
- [27] F. Lutscher, E. Pachevsky, and M.A. Lewis, *The effect of dispersal patterns on stream populations*, SIAM Rev. 478 (2005), pp. 749–7725.
- [28] J. Martin, *Derivation and investigation of mathematical models for spotting in wildland fire*, PhD thesis, University of Alberta, Canada, 2013.
- [29] J. Martin and T. Hillen, *The spotting distribution of wildland fires*, in preparation.
- [30] J.D. Murray, *Mathematical Biology. I: An Introduction*, 3rd ed., Springer-Verlag, New York, 2002.

- [31] H.G. Othmer, S.R. Dunbar, and W. Alt, *Models of dispersal in biological systems*, J. Math. Biol. 26 (1988), pp. 263–298.
- [32] PDE Solutions Inc., FlexPDE v.6.36, 2014. Available at <http://www.pdesolutions.com/>.
- [33] A. Potapov, U. Schlaegel, and M.A. Lewis, *Evolutionary stable diffusive dispersal*, 2014, submitted.
- [34] S.J. Pyne, P.L. Andrews, and R.D. Laven, *Introduction to Wildland Fire*, 2nd ed., John Wiley and Sons, New York, 1996.
- [35] J.G. Quintiere, *Fundamentals of Fire Phenomena*, John Wiley and Sons Ltd., Hoboken, NJ, 2006.
- [36] J. Smoller, *Shock Waves and Reaction-Diffusion Equations*, Springer Verlag, Berlin, 1982.
- [37] A.M. Syme, S.A. McQuarrie, J.W. Middleton, and B.G. Fallone, *Dosimetric model for intraperitoneal targeted liposomal radioimmunotherapy of ovarian cancer micrometastases*, Phys. Med. Biol. 48 (2003), pp. 1305–1320.
- [38] C. Tymstra, *Prometheus – the Canadian wildland fire growth model: Development and assessment*, Technical report, Canadian Forest Service, Northern Forestry Centre, 2007.
- [39] G. de Vries, T. Hillen, M. Lewis, J. Müller, and B. Schönfisch, *A Course in Mathematical Biology*, SIAM, Philadelphia, PA, 2006.
- [40] H. Yagista, *Existence and nonexistence of traveling waves for a nonlocal mono-stable equation*, Publ. Res. Inst. Math. Sci. 45 (2009), pp. 925–953.